

ENHANCED REDUCIBILITY OF Ni AND Ni + Pd IN ZEOLITE Y: BLOCKING OF SMALL CAGES WITH Ca^{2+} OR Mg^{2+} IONS

Jennifer S. FEELEY and Wolfgang M.H. SACHTLER

Ipatieff Laboratory and Department of Chemistry, Northwestern University, Evanston, IL 60208, U.S.A.

Received 15 March 1991; accepted 25 April 1991

Reducibility of zeolite encaged Ni^{2+} was found by temperature programmed reduction to increase in the following order $\text{Ni}/\text{NaY} < \text{Ni}/\text{MgY} < \text{Ni}/\text{CaY} < (\text{Pd} + \text{Ni})/\text{NaY} < (\text{Pd} + \text{Ni})/\text{MgY} < (\text{Pd} + \text{Ni})/\text{CaY}$. In comparison with NaY supported samples, bimetallic MgY and CaY supported samples exhibited enhanced Pd^{2+} and Ni^{2+} reducibility as well as higher $\text{H}_{\text{ads}}/\text{Me}^{\circ}$ ratios after reduction below 500°C . Temperature programmed reduction (TPR) and desorption (TPD) results indicate that Mg^{2+} and Ca^{2+} ions are occupying the small cages in the zeolite thus preventing the migration of the majority of Ni^{2+} and Pd^{2+} ions to these cages.

Keywords: Ni/Y zeolite, NiPd/Y zeolite, enhanced reducibility, MgY, CaY

1. Introduction

Reduction of Ni^{2+} ions in Y-zeolites is known to require a high temperature due to their preferential occupation of *small* zeolite cages [1–3]. Such high reduction temperatures (T_r) result in low Ni dispersions and, often, a bimodal distribution of the metal along with breakdown of the zeolite framework [4].

The dominant driving force for the migration of Ni^{2+} and other bipovalent ions in NaY to small cages is assumed to be Coulombic interaction. The density of negative charge is higher in small cages than in supercages; therefore a site occupancy is energetically favored with the bipovalent ions in the small cages, leaving monovalent Na^{+} ions in the large cages. In agreement with this rationale, our previous TPR and EXAFS results for Pd^{2+} in NaY, CaY and MgY have shown that after calcination Pd^{2+} ions are located in sodalite cages and hexagonal prisms in NaY, but in CaY and MgY they stay inside the supercages [5]. This difference in site occupancy resulted in a temperature programmed reduction (TPR) peak position 70°C lower for Pd/MgY and Pd/CaY than for Pd/NaY.

One should therefore expect that blocking of small cages with bipovalent ions such as Ca^{2+} or Mg^{2+} would also enhance the reducibility of Ni^{2+} ions in

Y-zeolites. Some results reported by Suzuki et al. [6,7] appear however at variance with this simple model. These authors reported a marked enhancement in Ni reducibility when the Na^+ ions in NaY were replaced by Ca^{2+} but no such effect was observed for Mg^{2+} . This leads to the question motivating the present research: Is the above model, that is merely based on simple electrostatic considerations, basically correct or are other factors involved which significantly differentiate between the two bipoisitive ions of similar size, viz. Ca^{2+} and Mg^{2+} ?

Additional motivation for the present study is based on recent results on co-reduction of (Pd + Ni)/NaY [8,9] and (Pd + Co)/NaY [10]. This work revealed the importance of proximity: i.e. only if the easily reducible ion (Pd^{2+}) and the less easily reducible ion (Ni^{2+} or Co^{2+}) are located in the *same* cage system will the former enhance the reducibility of the latter. This cation-cation interaction can take place in small or large cages, resulting after reduction either in atom pairs that are locked up in small cages or in easily growing bimetallic particles in supercages. Experimentally, both situations can be distinguished by measuring the adsorption of hydrogen, which is carried out by registering the temperature programmed desorption (TPD) profile after catalyst reduction and cooling to room temperature in hydrogen. It is known that transition metal clusters in supercages lead to a high $\text{H}_{\text{ads}}/\text{Me}^\circ$ ratio (Me° reduced metal atom); but for isolated atoms and pairs in small cages this ratio has been shown to be low [11]. The greatest enhancement in Ni reducibility, leading to the formation of small bimetallic PdNi_x particles in supercages, would therefore be expected for bimetallic samples where Pd^{2+} and Ni^{2+} ions co-occupy the supercages before reduction.

We therefore report on TPR and TPD studies of Ni in zeolite Y with secondary Na, Mg, Ca or Pd cations in the same zeolite.

2. Experimental

2(A). CATALYST PREPARATION

The CaY and MgY supports used in this study were prepared by an ion exchange/ion migration treatment of NaY, Linde LZY-52. Ion exchange was carried out for 24 hrs. at room temperature (RT) and $\text{pH} = 6.0$ using 0.01 M aqueous solutions of $\text{Ca}(\text{NO}_3)_2$ and $\text{Mg}(\text{NO}_3)_2$ in a 50% excess of the total exchange capacity of the zeolite. After ion exchange, the supports were washed with excess DDI water and then subjected to an "ion migration" [12] procedure in order to induce the migration of Ca^{2+} and Mg^{2+} ions to the small cages. This procedure consists of evacuation at room temperature for 12 hrs. followed by heating in vacuum to 500°C at a heating rate of 10°C per hour. The ion exchange/ion migration treatment was then repeated in order to maximize exchange of Ca^{2+} and Mg^{2+} ions for Na^+ ions. The resulting supports have the

following unit cell compositions as determined by chemical analysis: CaY: $\text{Ca}_{25}\text{Na}_6\text{Y}$ and MgY: $\text{Mg}_{20}\text{Na}_{16}\text{Y}$, where $\text{Y} = (\text{AlO}_2)_{56}(\text{SiO}_2)_{136} 244 \text{H}_2\text{O}$.

Three monometallic (Ni/NaY, Ni/CaY and Ni/MgY) and three bimetallic ((Pd + Ni)/NaY, (Pd + Ni)/CaY and (Pd + Ni)/MgY) samples were prepared by ion exchange of the supports described above with 0.01 M solutions of NiCl_2 and $\text{Pd}(\text{NH}_3)_4(\text{NO}_3)_2$. Bimetallic samples were prepared by co-exchange. Ion exchange was carried out for 24 hrs. at RT and $\text{pH} = 6$. The resulting samples have the following unit cell compositions: Ni/NaY: $\text{Ni}_{3.2}\text{Na}_{49.6}\text{Y}$, Ni/CaY: $\text{Ni}_{2.5}\text{Ca}_{23}\text{Na}_5\text{Y}$, Ni/MgY: $\text{Ni}_3\text{Mg}_{17.5}\text{Na}_{15}\text{Y}$, (Pd + Ni)/NaY: $\text{Pd}_{3.7}\text{Ni}_{3.0}\text{Na}_{42.6}\text{Y}$, (Pd + Ni)/CaY: $\text{Pd}_{3.85}\text{Ni}_{2.1}\text{Ga}_{19.8}\text{Na}_{4.5}\text{Y}$, (Pd + Ni)/MgY: $\text{Pd}_4\text{Ni}_{3.2}\text{Mg}_{13.2}\text{Na}_{15.2}\text{Y}$. Before temperature programmed experiments all samples were calcined in a high flow of ultra high purity O_2 (2 L/g catalyst/min) from RT to 500°C with a slow heating ramp ($0.5^\circ\text{C}/\text{min}$) and then held at 500°C for 2 hrs. This calcination procedure is known to completely oxidize the ammine ligands of Pd^{2+} [13].

2(B). TEMPERATURE PROGRAMMED REDUCTION (TPR) AND DESORPTION (TPD)

TPR and TPD experiments were carried out in a flow system described previously [14]. Rates of hydrogen consumption (TPR) and evolution (TPD) were monitored with a calibrated thermal conductivity detector. Following calcination, samples were purged at RT in UHP Ar for 20 min and then cooled to -78°C in Ar. *In situ* TPR profiles, figs. 1 and 2, were obtained following this pretreatment. The temperature was ramped from -55°C to 840°C at $8^\circ\text{C}/\text{min}$, and then held at 840°C until reduction returned to the baseline, in a 25 ml/min flow of 5% H_2/Ar .

Dispersions, expressed as $\text{H}_{\text{ads}}/\text{Me}^\circ$ ratios, of samples reduced to specific reduction temperatures, T_r , were obtained by running the following series of temperature programmed experiments: TPR1/TPD/TPR2. After calcination, samples were reduced, TPR1, to a specific T_r and then held at this T_r for 20 min. Samples were then cooled in the H_2/Ar mixture to RT and subsequently purged in ultra high purity Ar at RT for 20 min to remove the Pd hydride phase [15]. TPD in Ar (25 ml/min) was then carried out from -55°C to 760°C at $8^\circ\text{C}/\text{min}$. Following TPD, samples were cooled and a second TPR, TPR2, was collected to 760°C . Hydrogen consumption during TPR1 gives the amount of metal which is reduced before TPD, $\text{Me}^\circ = \text{reduced Pd} + \text{Ni}$. Hydrogen evolution during TPD is due to desorption of chemisorbed hydrogen, H_{ads} , and in some cases, to reoxidation of Ni° by zeolitic protons leading to Ni^{2+} and H_2 [9,12,16]. Previous data shows that Pd is not reoxidized under the conditions used in this work [9]. Hydrogen consumption in TPR2, therefore, is the sum of the reduction of any metal which was not reduced during TPR1, plus the reduction of any Ni which was reoxidized during TPD. From these measurements, and the Pd and Ni concentrations, $\text{H}_{\text{ads}}/\text{Me}^\circ$ ratios may be determined.

3. Results

3(A). TEMPERATURE PROGRAMMED REDUCTION

3(A)-1. Monometallic samples

The TPR profiles of Ni/NaY, Ni/MgY and Ni/CaY are presented in fig. 1. The extent of reduction of divalent Ni is determined by the integration of these profiles. In all samples Ni reduction was complete at 840°C. In table 1 the percentages of Ni reduced below 400°C and 600°C are presented. The main peak in the TPR profile of Ni/NaY, fig. 1a, is at ca. 840°C, with smaller peaks at ca. 460°C and 650°C, very similar to previous results on samples of higher Ni

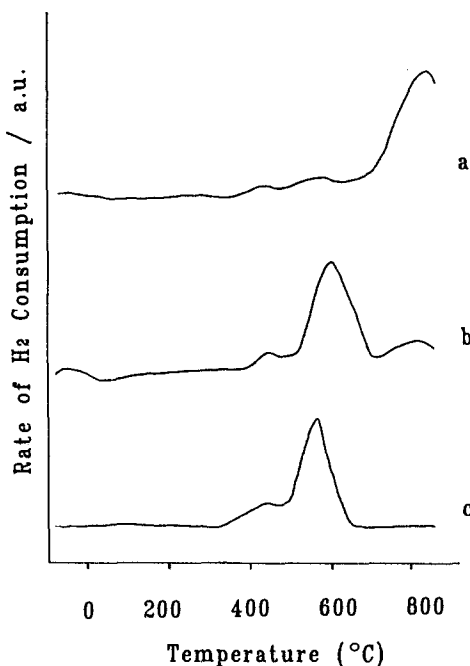


Fig. 1. TPR profiles of: a) Ni/NaY; b) Ni/MgY; c) Ni/CaY.

Table 1

Reducibility of Ni in mono and bimetallic samples ($T_c = 500^\circ\text{C}$)

Sample	Ni ²⁺ reduced (%)	
	below 400 °C	below 600 °C
Ni/NaY	—	14
Ni/MgY	5	41
Ni/CaY	6	84
(Pd + Ni)/NaY	24	31
(Pd + Ni)/MgY	55	80
(Pd + Ni)/CaY	70	100

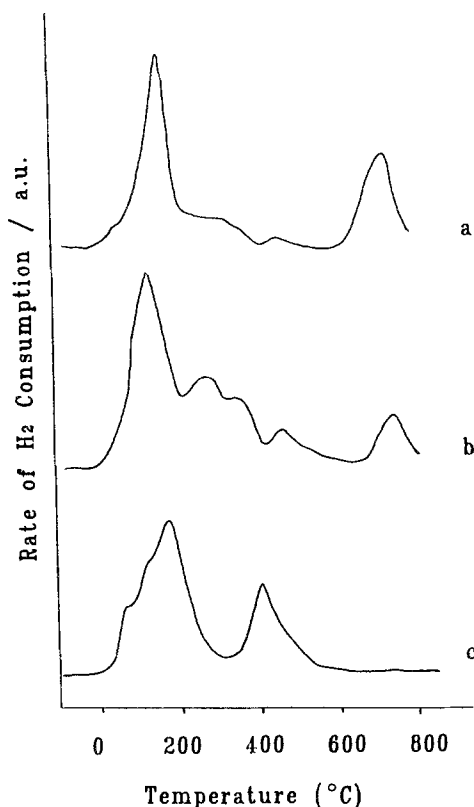


Fig. 2. TPR profiles of: a) (Pd + Ni)/NaY; b) (Pd + Ni)/MgY; c) (Pd + Ni)/CaY.

weight loading [7,9]. The Ni/MgY and Ni/CaY samples exhibit enhanced Ni reducibility when compared to Ni/NaY. The maxima of the main TPR peaks are at 610°C for Ni/MgY, fig. 1b, and at 570°C for Ni/CaY, fig. 1c. In addition, for Ni/MgY two small peaks at ca. 450°C and 830°C are observed, and for Ni/CaY a small peak is observed at 440°C. The positions of all Ni reduction peaks are higher in temperature however, than the reduction of NiO which occurs at ca. 330°C indicating that Ni^{2+} ions are ion exchanged into the cage system of the NaY, MgY, and CaY samples.

3(A)-2. Bimetallic samples

The TPR profiles of (Pd + Ni)/NaY, (Pd + Ni)/CaY and (Pd + Ni)/MgY are presented in fig. 2. Integration of these profiles corresponds to the complete reduction of Pd^{2+} and Ni^{2+} ions. In comparison with the TPR's of the monometallic Ni samples, it is clear that Pd dramatically enhances the reducibility of Ni in these bimetallic samples, as reported earlier for bimetallic NaY [9] and NaX [17,18]. In table 1 this effect is quantified for reduction below 400°C and 600°C.

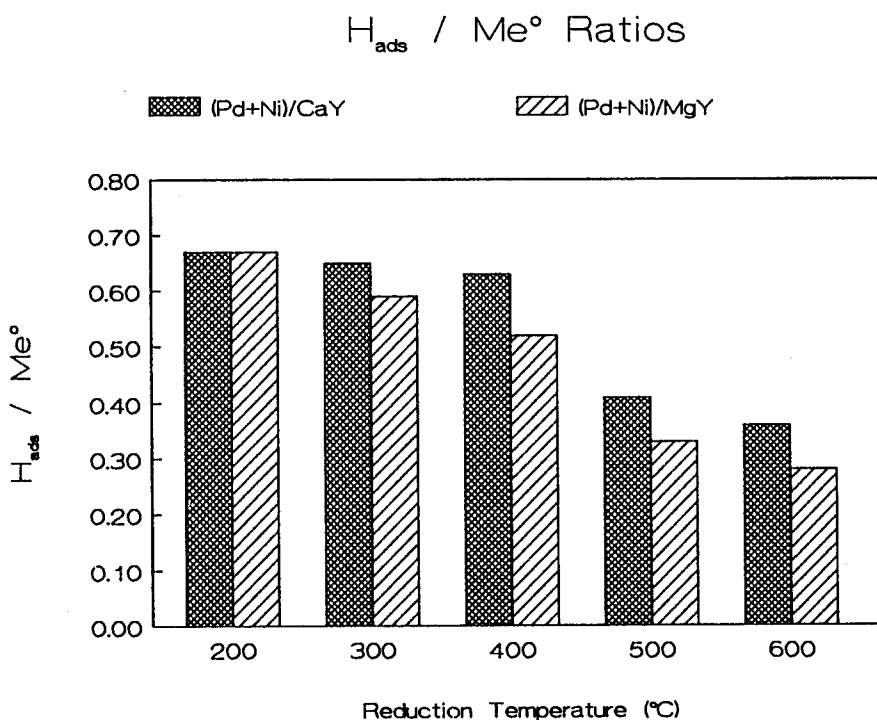


Fig. 3. $H_{\text{ads}}/\text{Me}^\circ$ ratios for (Pd+Ni)/MgY and (Pd+Ni)/CaY as a function of reduction temperature, T_r .

Ni reduction above ca. 600 °C can be attributed to reduction of Ni^{2+} ions inside the small cages. The (Pd + Ni)/CaY sample is the only one out of the three bimetallic samples where Ni reduction is complete below 600 °C. In contrast, high temperature peaks at 710 °C and 730 °C are observed for (Pd + Ni)/MgY and (Pd + Ni)/NaY respectively. As found previously [9], these high temperature Ni TPR peaks are shifted to lower temperatures in bimetallic samples, ie. maxima are observed at 830 °C and 840 °C for Ni/MgY and Ni/NaY respectively. Less reduction above 600 °C occurs in (Pd + Ni)/NaY than in Ni/NaY. This trend is reversed for the MgY support.

3(B). $H_{\text{ads}}/\text{Me}^\circ$ ratios

In fig. 3 the $H_{\text{ads}}/\text{Me}^\circ$ ratios are plotted as a function of T_r for bimetallic (Pd + Ni) supported on CaY and MgY. For a given T_r , the $H_{\text{ads}}/\text{Me}^\circ$ values of these two samples are similar though slightly higher for the CaY support. For both samples the $H_{\text{ads}}/\text{Me}^\circ$ ratio monotonically decreases with increasing T_r . This result is in contrast with previous findings for Pd [11] and (Pd + Ni) [9] supported on NaY and calcined to the same temperature, 500 °C. For these NaY supported samples the $H_{\text{ads}}/\text{Me}^\circ$ ratios were found to pass through a maximum with increasing T_r ; the maxima are located at $T_r = 300$ °C for Pd/NaY and at

$T_r = 500^\circ\text{C}$ for (Pd + Ni)/NaY. Reoxidation of Ni by reaction with zeolitic protons was found to occur during TPD, similar to previous findings for NaY samples [9].

For monometallic Ni/CaY and Ni/MgY high T_r 's were necessary to achieve substantial Ni reduction. The $H_{\text{ads}}/\text{Me}^\circ$ ratios: 0.18 and 0.16 respectively after $T_r = 600^\circ\text{C}$, are lower than for the corresponding (Pd + Ni) samples treated under the same conditions, fig. 3. Low Ni reducibility and low dispersion have been frequently reported for Ni/NaY samples [4,6,9,12].

4. Discussion

4A. EFFECT OF Ca^{2+} AND Mg^{2+} ON Ni REDUCIBILITY

In both the CaY and MgY samples the substitution of divalent Ca^{2+} and Mg^{2+} ions for Na^+ ions has resulted in significant enhancements in the reducibility of Ni^{2+} ions, as is obvious from the TPR results in figs. 1 and 2. The main TPR peaks are 270°C and 230°C lower for Ni/CaY and Ni/MgY respectively than for Ni/NaY. The main peaks in both samples occur close to the temperature, 540°C , where reduction of Ni^{2+} located in the supercages has previously been reported [7]. These results indicate that for the CaY and MgY supports, Ni^{2+} ion migration to the small cages has been minimized by the preferential occupation of these cages by Ca^{2+} and Mg^{2+} ions.

Suzuki et al. studied the reducibility of Ni^{2+} in CaY and MgY samples using higher Ni weight loadings [6,7]. They concluded that Ca^{2+} ions are much more effective as site blocker ions than Mg^{2+} ions. However, for the low Ni concentrations used in this work, a different result is found: Ca^{2+} and Mg^{2+} exert very similar effects. These ions appear to be efficient site blockers and the majority of Ni^{2+} ions remain in the supercages. For efficient site blocking it is, of course, essential, that the bipoisitive ions are located in the small cages. The ion exchange/ion migration procedure used in this work; along with the careful control of pH (in order to prevent $\text{Mg}(\text{OH})_2$ formation) may have resulted in a higher concentration of Mg^{2+} ions in the small cages than in Suzuki's work.

The fact that the concentration of Ni^{2+} in the small cages appears to be somewhat greater for MgY than for CaY samples in this work could be due to the less complete exchange of Mg^{2+} than that of Ca^{2+} for Na^+ ions in CaY. This could result in a higher concentration of Na^+ ions in the small cages, which Ni^{2+} ions could exchange for during calcination. However, the possibility that Ni^{2+} ions are able to replace some Mg^{2+} ions in the small cages can not be ruled out. It is clearly less favorable however, for a Ni^{2+} ion to replace a Mg^{2+} or Ca^{2+} ion that has been chased to a small cage, than it is for a Ni^{2+} ion to successfully compete with one of these ions for initial occupancy of this cage.

As mentioned in the introduction, the greatest enhancement in Ni reducibility would be expected for samples where Ni and Pd occupation of small cages is minimized and Ni^{2+} and Pd^{2+} ions co-occupy supercages. The (Pd + Ni)/CaY sample studied in this work gives evidence that under these ideal conditions, all Ni^{2+} can be reduced below 600 °C.

4B. EFFECT OF SITE BLOCKER IONS ON PARTICLE GROWTH MECHANISM

The presence of Ca^{2+} or Mg^{2+} ions not only enhances the reducibility of Ni^{2+} and Pd^{2+} but also effects the particle growth mechanism.

When ions (Pt [19], Pd [20], Ni[21]) occupy the small cages after calcination, reduction results initially in the formation of isolated atoms or dimers in these small cages. As these species are unable to chemisorb hydrogen [19–22], the dispersion, defined by the $H_{\text{ads}}/\text{Me}^\circ$ ratio is low. At higher T_r 's, particles in the supercages are formed via the activated migration of escaping atoms from the small cages. Accordingly, TPD studies have shown that the $H_{\text{ads}}/\text{Me}^\circ$ ratio passes through a maximum as a function of T_r [11].

In this study, where migration of ions to the small cages is minimized by the presence of site blocker ions, the interaction of Pd^{2+} and Ni^{2+} ions occurs in the supercages leading to the formation of small bimetallic PdNi_x particles at low T_r . From the TPR results it is clear that a significant fraction of Ni is reduced along with Pd in the lowest temperature peak. Recent findings suggest that similar mutual enhancements in Pd and Ni reducibility occur, leading to bimetallic particle formation, when these ions co-occupy the small cages of NaY [8]. However, due to retention of reduced PdNi dimers in the small cages, much higher reduction temperatures, ie. 500 °C, were required to form small PdNi_x particles in the supercages of NaY. In the present bimetallic CaY and MgY samples, Pd^{2+} and Ni^{2+} ions are located, almost exclusively, in the supercages. As would be expected for these samples no maximum is observed in the $H_{\text{ads}}/\text{Me}^\circ$ ratios as a function of T_r ; the dispersion of the PdNi_x particles simply decreases with increasing T_r .

Clearly the particle formation mechanism for (Pd + Ni)/CaY and (Pd + Ni)/MgY, is more similar to that observed for monometallic Pd/NaY, where careful pretreatment conditions were chosen to maintain $\text{Pd}(\text{NH}_3)_2^{2+}$ ions in the supercages before reduction. In this case a similar decrease in dispersion with increasing T_r was reported [11]. The similarity of (Pd + Ni)/NaY with Pd/NaY justifies the conclusion that the overwhelming majority of the initial metal particles, after reduction at low temperature, is located in supercages, not at the external zeolite surface. In addition, the reaction of encaged Ni° with zeolitic protons during TPD has been observed in this work. EXAFS data showed that reduction of supercage based $\text{Pd}(\text{NH}_3)_2^{2+}$ ions at low T_r leads to the initial formation of Pd_4 and Pd_6 clusters, which upon exposition to CO, agglomerate to $\text{Pd}_{13}(\text{CO})_x$ clusters [23]. This agglomeration is entirely determined by the width of

the windows between supercages, as follows from comparison with Pd/Na5A where, under identical conditions, $\text{Pd}_6(\text{CO})_y$ is formed [24]. At higher reduction temperature, however, the zeolite matrix loses its rigidity and larger particles are formed, some of which might be located in voids or at the external surface.

5. Conclusions

Ca^{2+} and Mg^{2+} ions have been shown to effectively prevent the migration of Pd^{2+} and Ni^{2+} ions to the small cages of Y-zeolite. Interaction between Pd^{2+} and Ni^{2+} ions in the supercages leads to significant enhancements in Ni reducibility and the formation of highly dispersed PdNi_x particles in the supercages. The reducibility and dispersion of these samples are much higher than for bimetallic NaY samples where Pd^{2+} and Ni^{2+} ions co-occupy small cages before reduction.

Acknowledgements

We gratefully acknowledge support from the U.S. Department of Energy, grant number DE-FG02-87ERA3654.

References

- [1] D.H. Olson, J. Phys. Chem. 72, No. 13 (1968) 1538.
- [2] P. Gallezot and B. Imelik, J. Phys. Chem. 77, No. 5 (1973) 652.
- [3] M. Briend-Fraure, J. Jeanjean, M. Kermarec and D. Delafosse, J. Chem. Soc., Faraday Trans. I, 74 (1978) 1538.
- [4] P.A. Jacobs, H. Nijs, J. Verdonck, E.G. Derouane, J.P. Gibson and A.J. Simoons, J. Chem. Soc., Faraday Trans. I, 75 (1979) 1196.
- [5] Z. Zhang, T. Wong and W.M.H. Sachtler, J. Catal. 128 (1991) 13.
- [6] M. Suzuki, K. Tsutsumi and H. Takahashi, Zeolites 2 (1982) 51.
- [7] M. Suzuki, K. Tsutsumi, H. Takahashi and S. Yasukazu, Zeolites 9 (1989) 98.
- [8] J.S. Feeley and W.M.H. Sachtler, Zeolites 10, No. 8 (1990) 738.
- [9] J.S. Feeley and W.M.H. Sachtler, J. Catal., submitted.
- [10] Z. Zhang, W.M.H. Sachtler and S. Suib, Catal. Lett. 2 (1989) 395.
- [11] S.T. Homeyer and W.M.H. Sachtler, J. Cat. 118 (1989) 266.
- [12] H.J. Jiang, Effects of metal additives on reducibility and dispersion of Ni/NaY catalysts, PhD. Thesis, Northwestern University, Evanston, IL, 1988.
- [13] S.T. Homeyer and W.M.H. Sachtler, J. Catal. 117 (1989) 91.
- [14] S.H. Park, M.S. Tzou and W.M.H. Sachtler, Appl. Catal. 24 (1986) 85.
- [15] H.S. Hwang and M. Boudart, J. Catal. 39 (1975) 44.
- [16] H.J. Jiang, M.S. Tzou and W.M.H. Sachtler, React. Kin. Catal. Lett. 35 (1987) 207.
- [17] M.F. Guilleux, M. Kermarec and D. Delafosse, J. Chem. Soc., Chem. Comm. (1977) 102.
- [18] M.F. Guilleux and D. Delafosse, J. Chem. Soc., Faraday Trans. I, 175 (1979) 165.

- [19] P. Gallezot, A. Alarcon-Diaz, J.A. Dalmon, A.J. Renouprez and B. Imelik, *J. Catal.* 39 (1975) 334.
- [20] G. Bergeret, P. Gallezot and B. Imelik, *J. Phys. Chem.* 85 (1981) 411.
- [21] M. Suzuki, K. Tsutsumi and H. Takahashi, *Zeolites* 2 (1982) 185.
- [22] P. Gallezot and B. Imelik, *Adv. Chem. Ser.* 121 (1973) 66.
- [23] Z. Zhang, H. Chen, L.L. Sheu and W.M.H. Sachtler, *J. Catal.* 127 (1991) 213.
- [24] Z. Zhang and W.M.H. Sachtler, *J. Molec. Catal.*, accepted.